Jurnal Polimesin
Department of Mechanical Engineering
State Polytechnic of Lhokseumawe
http://e-jurnal.pnl.ac.id/polimesin

e-ISSN : 2549-1999 No. : 3 Month : June
p-ISSN : 1693-5462 Volume : 24 Year : 2026

Processing dates: received on 2026-03-26, reviewed on 2026-4-05, accepted on 2026-04-28 and online availability on 2026-06-30

Evaluation of hardness and dry sliding wear performance of Al/BA-silica sand composites as brake friction materials.

Sukanto[1*], Erwanto[1], Husman[1], Erwansyah[1], Rodika[1], Yudi Oktriadi[1], Eko Yudo[1], Ardiansyah[2].
[1]Department of Mechanical Engineering, Bangka Belitung State Manufacturing Polytechnic, Sungailiat 33211, Indonesia
[2]Mechanical and Manufacturing Engineering Study Program, Bangka Belitung State Manufacturing Polytechnic, Sungailiat 33211, Indonesia
*Corresponding author: sukanto.wiryono@gmail.com

Abstract
As many as 70 countries have banned the use of asbestos-based materials because its fine, lightweight fibers are easily inhaled by humans, causing lung cancer, particularly mesothelioma, which can be fatal. This study aims to determine the effect of a silica sand and boiler ash reinforcement alloy on the application of non-asbestos aluminum matrix composite brake pads. This research uses a powder metallurgy method with varying reinforcement weight ratios, namely 8%, 10%, 12%, and 14% by weight. The mixing process is carried out through mechanical alloying using a horizontal ball mill at 90 rpm with a BPR ratio of 10:1. Hot compaction at 300°C was varied at a pressure of 5000-5300 PSI, followed by sintering at 580°C. Density, hardness, and wear were tested using ASTM standards, which were then compared with the brake lining standard SNI-09-0143-1987. Microstructural characterization was performed using SEM to determine the extent of interlocking bonds in the composite. The results showed that the 12wt% composition at 5200 PSI produced the best properties, with a density of 2.121 g/cm³, a hardness of 93.628 HB, and a wear of 0.0193 mm³/Nm. SEM images showed more uniform interlocking bonds compared to other variations. Increasing the compaction pressure was proven to increase density, hardness, and wear resistance. Overall, this study successfully produced environmentally friendly composite brake linings based on Silica Sand Powder and Boiler Ash without using asbestos materials.

Keywords:
Boiler ash, composite, non asbestos brake pads, powder metallurgy, silica sand

1 Introduction

A total of 72 countries have officially banned the use of various asbestos-based materials in various industrial applications [1]. This policy was implemented due to the very serious health impacts and has been scientifically proven to endanger human safety. In Indonesia alone, approximately 1,600 deaths are recorded each year associated with diseases caused by asbestos exposure, while globally the number of victims reaches approximately 200,000 people per year. These figures indicate that asbestos exposure remains a significant public health problem and requires serious attention at the national and international levels [2]. Asbestos material is known to produce microscopic fibers that are very fine and light so that they are easily released into the air and float for a long time. The diameter of these fibers is around 0,2 µm, or less than 1/700 the diameter of a human hair, so these particles are very easy to inhale without realizing it [3]. When accumulated in the respiratory tract, asbestos fibers can trigger serious health problems, one of which is mesothelioma. This aggressive lung cancer is estimated to cause around 230,000 deaths annually worldwide [4][5]. These risks include esophageal cancer, mesothelioma, gastric cancer, colorectal cancer, and several autoimmune diseases [6]. In response to these issues, practitioners and researchers in the fields of materials engineering and the automotive industry continue to strive to develop alternative materials that can replace asbestos in brake lining friction materials, known as Non-Asbestos (NOB) Brake Pad [7]. One emerging innovation is a composite designed as a substitute for asbestos-based brake linings, namely Aluminum Matrix Composite (AMC) [8].

Aluminum is the second most widely used metal in the world after iron and steel. Its high utilization is due to its numerous superior physical and mechanical properties compared to other metals. One of its main advantages is its significantly lighter weight, with a density of approximately 2.7 g/cm³, which is only one-third the density of alloy steel or copper. Despite its light weight, aluminum does not necessarily mean low strength [9]. Through composition engineering and specific treatments, aluminum alloys can achieve tensile strengths equivalent to steel. With these characteristics, aluminum alloys can produce structures that remain strong and rigid while having a relatively low mass [10]. This combination of adequate mechanical strength and light weight makes aluminum ideal for applications that demand weight efficiency without sacrificing structural performance. Therefore, this material is widely used in the mobile vehicle industry, including marine fleets, land vehicles, and aircraft [11]. Even recycled aluminum from scrap can be reused as a composite matrix without significantly reducing its performance potential. This further strengthens aluminum's position as a strategic material in the development of modern, efficient, economical, and sustainable composites [12]. In addition to aluminum matrix composites, phenolic resin matrix composites have also been widely developed recently, with a temperature maximum of approximately 350 ºC [13], which can be increased to 480 ºC when the phenolic matrix is combined with Boron [14]. Although this temperature is lower than that of aluminum matrix composites, it is sufficient for motorcycle brake pads and complies with SNI 09-0143-1987 [15] or SNI 09-4404-2008 [16].

Powder Metallurgy (PM) technology is widely used in manufacturing processes these days because this method offers several advantages over other manufacturing techniques [17]. One of its main advantages is its very high raw material efficiency, with approximately more than 95% of the material being recovered into the final product, thus minimizing production waste. Furthermore, this technology is highly suitable for producing small components, even with complex geometries and high precision. The production process can also be carried out at relatively lower temperatures than casting methods, thus saving energy and reducing the potential for material degradation. In general, Powder Metallurgy technology consists of three main stages: composite powder mixing, compaction, and sintering [18]. The mixing stage is carried out using the Mechanical Alloying method, a process in which powder particles undergo repeated cold welding, fracturing, and re-welding in a high-energy ball mill. This mechanism allows for plastic deformation and a more homogeneous particle distribution [19]. The Mechanical Alloying method has been widely applied due to its ability to produce a more uniform powder mixture while simultaneously grinding or crushing the particles. This process also promotes mechanical alloying through repeated cold-welded cycles, resulting in more intensive inter particle interactions and a more uniform distribution of reinforcement within the matrix [20]. Next, the Aluminum Matrix Composite (AMC) is compacted using a hot pressing method to enhance the wetting ability of the matrix to the reinforcement particles [17]. The final stage is the AMC sintering process, which is generally carried out at a temperature range of approximately 70% to 90% of the matrix's melting temperature. Under these conditions, inter particle diffusion occurs, strengthening

bonds and increasing densification without causing complete melting of the matrix [20].

This AMC reinforcement can be achieved using various metal powders, such as iron, steel, copper, bronze, and combined with ceramic or non-metallic carbon powder [21]. In addition, this composite reinforcement can also be done by combining it with agricultural waste materials, such as Rice Husk Ash (RHA) powder [22]. Baggase Ash (BA) powder [23] and wastes of coal combustion products (fly ash, boiler ash, flue gas desulfurization gypsum and bottom ash) [24] which are abundant in Indonesia and therefore more economical. In general, Fly Ash waste contains ceramic compounds such as alumina (Al_2O_3) and silica (SiO_2), which originate from the coal and palm oil processing industries, gypsum flue-gas desulfurization, and Fly Ash [25]. Fly Ash is widely used as a reinforcement because it can improve mechanical properties such as strength/toughness, stiffness, hardness, abrasion resistance, and low density. It exhibits Coefficient of Thermal Expansion, CTE values that decrease with the addition of Fly Ash [26]. Apart from Fly Ash, metal oxide powder in the form of Silica Sand tailings, a mineral with a very high SiO_2 content of at least 90% [27] is also very good for use as a reinforcement in Aluminum Matrix Composites. In general, SiO_2 is in the form of a compound that often combines as $ZrSiO_4$ [28]. Furthermore, silica sand reserves in Indonesia are abundant [29] and offer several advantages, including low density, high temperature resistance, hardness, and high wear resistance [30]. So, Silica Sand Powder is suitable for use as a reinforcement in aluminum matrix composites which require good hardness and friction resistance [31].

Several previous studies have been conducted, using AMC and BA as reinforcements which showed good mechanical properties, especially density, hardness, and wear rate, as a comparison in this study as described below. Choudhury [26] applied 12.5% BA as reinforcement, while Subarmono [32] applied 10%, where the results of Subarmono's research showed higher density, hardness and wear rate values than Choudhury's research. Furthermore, AMC research using Silica Sand Powder as reinforcement has been conducted by Daniel-Mkpume [33] and Shaikh [34] with a composition of 10% reinforcement, respectively, producing densities of 2.6 and 2.48 g/cm3, hardness of 150 and 63 HB and wear rate No-Available and 0.000685 mm^3/mm. Referring to the description above, it turns out that there has been no specific research that examines the use of reinforcement in the form of a mixture consisting of Boiler Ash (BA) and Silica Sand Powder (SiO_2), which uses a Recycled Aluminum Matrix for brake lining applications. Therefore, this paper discusses the development of a Recycled Aluminum Matrix Composite reinforced with a mixture of Boiler Ash and Silica Sand Powders, with the main focus on the evaluation of mechanical properties, is very promising as a superior new discovery in the field of Non-Asbestos Brake linings that are more economical and environmentally friendly.

Conventional anti-tank weapons such as LRAC (Lance-Roquettes Antichar), Instalaza C90-CR, and Armbrust have proven effective in combat operations. However, their high operational costs, single-use ammunition, and complex logistics limit their applicability for routine training activities [2], [3]. These constraints have encouraged the development of cost-effective training platforms that can replicate operational conditions while reducing expenditure and logistical burden.

Pneumatic propulsion systems have been introduced as sustainable alternatives to CTW training by using compressed gas rather than solid propellants. These systems enable repeated use, improved operational safety, and reduced environmental impact. Nevertheless, preliminary field tests of pneumatic CTW trainers indicate that significant recoil forces remain, reaching approximately 80 N at a working pressure of 30 bar, which negatively affects weapon stability, shooter posture, and firing accuracy.

Existing recoil-mitigation techniques, including mechanical dampers, recoil springs, and buffer systems, were originally designed for solid-propellant weapons characterized by short-duration and high-peak impulse loads. In contrast, pneumatic systems produce longer-duration, lower-peak, but higher-total-impulse profiles. This mismatch causes conventional mitigation devices to provide insufficient damping or to require additional mass and structural reinforcement, thereby reducing portability and operational practicality.

Several previous studies have attempted to improve launcher stability and recoil control through structural reinforcement and mass optimization [6], pressure-loss management [7], airflow regulation using vortex tubes [8], rigid pneumatic launcher designs [9], and lightweight composite structures combined with telemetry systems [10]. However, most of these approaches rely on increased structural stiffness, additional components, or complex flow-control mechanisms, thereby increasing system complexity and maintenance requirements while failing to address dynamic recoil-impulse mitigation in pneumatic CTW trainers directly.

Furthermore, existing studies have primarily focused on propulsion efficiency, structural durability, or material optimization, with limited attention to integrated recoil control mechanisms specifically optimized for training launchers. Quantitative evaluations of recoil reduction via internal momentum transfer mechanisms in pneumatic CTW systems are scarce, indicating a clear research gap in this field.

To address this gap, the present study investigates the design and implementation of a collision-based counter-recoil mechanism integrated into the valve lever assembly. The proposed system employs a counter pad that generates controlled impact with the valve housing during gas release, producing forward momentum to counteract rearward recoil forces. This study systematically evaluates the influence of pressure levels and counter pad mass on recoil behavior using experimental testing and statistical analysis. The novelty of this research lies in the application of an internal collision-based momentum transfer mechanism that provides effective recoil mitigation without requiring additional external components or major structural modifications, while simultaneously maintaining or improving projectile range performance.

The findings of this research advance indigenous defense training technology by providing validated design parameters for safer, more ergonomic CTW trainers. Moreover, this study supports the development of reliable and cost-effective training systems that enhance skill transfer, operational readiness, and long-term sustainability for military personnel.

2 Research methodology

2.1 Material

This research was conducted using an experimental method, using recycled aluminum metal powder as the matrix, with an average particle size of 282.53 µm according to the Particle Size Analyzer (PSA) test. Based on chemical composition analysis, the powder was predominantly composed of aluminum at 83.4%, accompanied by other elements such as silicon 10.09%, copper 2.6%, nickel 1.042%, zinc 0.849%, iron 0.640%, and approximately 1.379% of other elements in small amounts. This composition indicates that the base material used was a recycled aluminum alloy with significant silicon content. The added reinforcing powder consisted of a mixture of silica sand derived from tin tailings and Boiler Ash (BA), a waste product from the palm oil industry. The main compounds of Silica Sand Powder include 81% SiO_2, 12% FeO_2, 5% TiO_2, and 2% ZrO_2. Meanwhile, Boiler Ash has a maximum SiO_2 content of 63.4%, with the remaining components being oxides such as Al_2O_3 and Fe_2O_3 in certain proportions. The three types of powders, recycled aluminum, silica sand, and boiler Ash were tested for Particle Size Distribution using PSA at the Laboratory of the Faculty of Mathematics and Natural Sciences, Brawijaya University, Malang. The test results showed D50 values for aluminum, silica sand, and Boiler Ash of 283 µm, 168 µm, and 156 µm, respectively, indicating that the reinforcement particles are finer than the aluminum matrix.

This experimental study used a full factorial design method, consisting of two factors with four levels each. Each sample was replicated three times, resulting in a total of 48 samples. The

reinforcement variable factors were less than 20% to avoid clumping [35] respectively, 14%, 12%, 10%, and 8%, while the compaction pressure variable factors were 5000, 5100, 5200, and 5300 PSI, referring to Kumar's research [36]. This research was conducted by applying Powder Metallurgy technology, including the following processes: powder mixing process, compaction process and sintering process, and continued with several testing and analysis processes, as explained below.

2.2 Mixing with mechanical blending

The Powder Metallurgy (PM) process begins with the powder mixing stage, which in this study was conducted using the Mechanical Alloying (MA) system to combine the matrix powder and the reinforcement powder for greater homogeneity [20]. Before mixing with the matrix, the reinforcement powder is first prepared, consisting of two components: Silica Sand and Boiler Ash. The two reinforcement powders are mixed using a mixer at a 1:1 weight ratio to achieve an even mixture distribution before entering the mechanical alloying stage. Next, the MA process between the matrix powder and the reinforcement powder mixture is carried out with operational parameters of a machine rotation speed of 90 rpm for 6 hours, and a Ball-to-Powder Ratio (BPR) of 10:1, using Horizontal Ball Mill equipment made by αβγ Laboratory, Landungsari Malang. These parameters are set with reference to the critical speed of the ball mill and with reference to the MA process parameters to obtain a more optimal alloy. [10]. The equipment used is a Radial Ball Mill driven by a 0.5 HP electric motor. The matrix composition variations applied in this mixing process consist of four weight fractions: 86%, 88%, 90%, and 92%, which correspond to reinforcement additions of 14%, 12%, 10%, and 8%, respectively. The results of the MA process carried out at the Polman Babel Mechanical Workshop Laboratory were then analyzed for particle size using a Particle Size Analyzer (PSA) at the Laboratory of the Faculty of Mathematics and Natural Sciences, Brawijaya University, Malang. Based on the results of the PSA test after the MA process for 6 hours, the average particle size (D50) was obtained sequentially as follows: 88% matrix composition produced a D50 of 117 µm; 90% matrix produced a D50 of 118.37 µm; 92% matrix produced a D50 of 122 µm; and 94% matrix produced a D50 of 120.41 µm.

2.3 Hot compaction

The second stage in the Powder Metallurgy (PM) process is hot compaction, which aims to shape and compact the powder mixture from Mechanical Alloying into a workpiece with initial strength before sintering [17] [10]. This process is carried out at the Polman Babel Mechanical Workshop Laboratory using a WIPRO hydraulic press with a maximum capacity of 50 tons. During the compaction process, the mold temperature is maintained at 300°C and the pressure is held for 10 minutes to ensure optimal compaction and enhance inter particle bonding. The mold used is a ring-shaped mold with an outer diameter of 50 mm and an inner diameter of 20 mm, ensuring the resulting specimens have an annular geometry as required for testing. Sample thickness is controlled by the amount of MA powder mixture injected into the mold, which is approximately 35 grams for each specimen. This amount results in a minimum ring thickness of approximately 8 mm, which meets the requirements of the ASTM E110 standard [37]. In this study, varying compaction pressures were applied to analyze their effect on densification and the mechanical properties of the composites. Four pressure levels were used in stages, namely 5000, 5100, 5200, and 5300 PSI, to identify the optimum pressure capable of producing the best density and structural quality in the hot compacted specimens.

2.4 Sintering

The third stage in the Powder Metallurgy (PM) process is sintering, a heat treatment that aims to increase material density, reduce porosity, and eliminate any internal stresses remaining after the compaction process [38]. Through this process, the compacted powder particles undergo atomic diffusion at high temperatures, forming stronger and more stable bonds [39]. Furthermore, sintering also serves to repair and strengthen the interlocking bonds between the matrix powder and the reinforcement powder, resulting in a more homogeneous composite structure with improved mechanical integrity [40]. The sintering process was carried out using a Nabertherm N161/13 oven at 580°C with a holding time of 10 minutes. After the heating stage was completed, the specimen was not immediately removed but rather slowly cooled in the oven for at least 24 hours. This gradual cooling was carried out to prevent rapid temperature changes (thermal shock), which could cause microcracking or even structural failure. In general, aluminum matrix composite specimens are very sensitive to thermal shock, so controlling the cooling rate is an important factor in maintaining the quality and integrity of the sintered material.

2.5 Testing and analysis methods

The analysis in this study was conducted by comparing the results of physical and mechanical property tests, including density, hardness, and wear resistance, each based on the relevant ASTM standards: ASTM E110 for hardness [37], ASTM B962-17 for density [41] and ASTM G99-17 for wear [42]. These tests aimed to quantitatively evaluate the composite performance and determine the effect of process variations on the quality of the resulting material. Furthermore, the physical test results were corroborated through microstructural characterization using scanning electron microscopy (SEM) images conducted at the Polytechnic ATMI Surakarta to observe the microstructure and particle distribution within the specimens.

Density testing was conducted based on Archimedes' principle, by weighing the specimens in air-dry conditions and submerged in distilled water [43]. The sample density (ρm) was calculated using an equation involving the sample's dry weight (ms), wet or submerged weight (mg), and the density of distilled water (ρH_2O) as a reference fluid, following equation (1). This method allows for the determination of actual density while also providing an indication of the material's porosity level.

Meanwhile, a quantitative description of the material's resistance to friction and mass loss during the testing process is calculated by referring to equation (2), the volume of abraded material (W) based on the geometric parameters of the wear trace, with the thickness of the rotating disc (B), the width of the wear gap (b), and the radius of the disc (r), according to the equation used. To obtain the volumetric wear rate (V) by referring to equation (3), the volume of material released (W) is then compared with the total sliding distance (x) [43].

$$m = \frac{ms}{ms - mg}\ \rho H_2O \quad (1)$$

$$W = \frac{Bb^3}{12r} \quad (2)$$

$$V = \frac{w}{x} = \frac{B\ b^3}{12\ r.x} = \frac{m}{\rho\ .x} \quad (3)$$

3 Result and discussion

3.1 Density

Based on the collection of density test data, in accordance with ASTM B962-17 [41], samples are weighed in air and then in water, using density test equipment made by αβγ Laboratory, Landungsari Malang. Each sample was weighted three times, with a deviation of ±0,05 grams. The results are then calculated using equation (1) and presented in Figure 1. NOB Brake Pad Composite Density Chart, a graph was created as shown in Fig.1, indicating that density increases with increasing reinforcement percentage up to a maximum at a

reinforcement composition of 12wt%, then decreases slightly at a density with a reinforcement composition of 14wt%

Table 1. Density values for NOB brake pad composites

No.	Reinforcement Percentage [%]	Compaction [PSI]	Average [grams/cm³]
1	8	5000	1,716
2	8	5,100	1,800
3	8	5,200	1,865
4	8	5300	1,921
5	10	5,000	1,846
6	10	5100	1,913
7	10	5,200	1,908
8	10	5300	1,960
9	12	5,000	1,882
10	12	5100	1,945
11	12	5,200	2,121
12	12	5,300	2,106
13	14	5,000	1,929
14	14	5,100	1,891
15	14	5,200	2,009
16	14	5,300	2,004

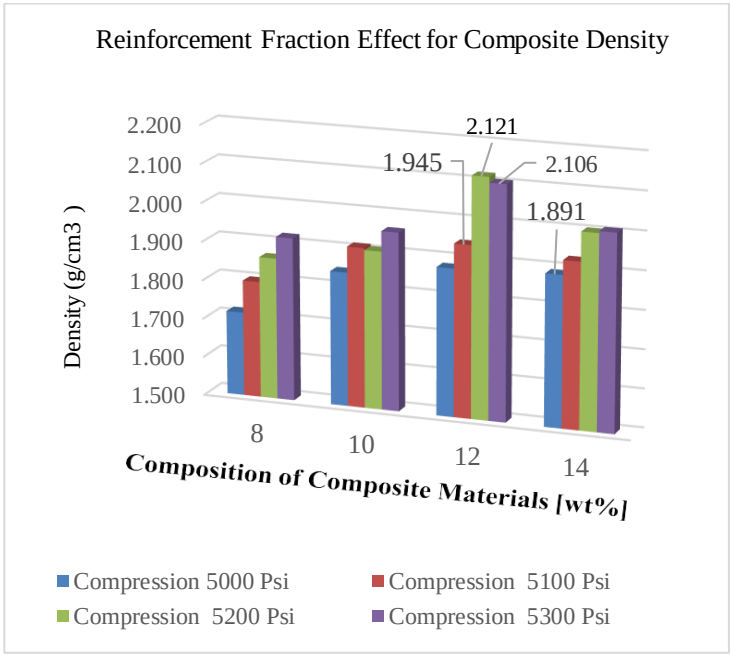

Fig. 1. NOB brake pad composite density chart

3.2 Hardness

Hardness testing was conducted using a Portable Brinell hardness tester, ZwickRoell Brinell brand, in accordance with ASTM E110 [37] This test was conducted several times, and the three results with deviation ± 3 HB were selected. Based on the test data and the calculation results, the following graph was created as shown in Fig.2. Graph of Non-Asbestos Brake Pad Composite Hardness. As with density, the hardness test results also showed a similar trend: the higher the reinforcement, the higher the hardness, up to a reinforcement composite composition of 12wt%. However, when the percentage of reinforcement was increased, the hardness properties were reversed, decreasing slightly when the reinforcement was added up to a composite material composition of 14wt%.

Table 2. NOB brake pad hardness values [HB]

No.	Reinforcement Percentage [%]	Compaction [PSI]	Average (HB)
1	8	5000	75,688
2	8	5,100	78,899
3	8	5,200	81,741
4	8	5,300	83,510
5	10	5,000	77,293
6	10	5,100	83,373
7	10	5,200	84,847
8	10	5,300	86,177
9	12	5,000	80,407
10	12	5,100	85,575
11	12	5,200	93,628
12	12	5,300	88,863
13	14	5,000	77,792
14	14	5,100	80,832
15	14	5,200	82,269
16	14	5,300	82,160

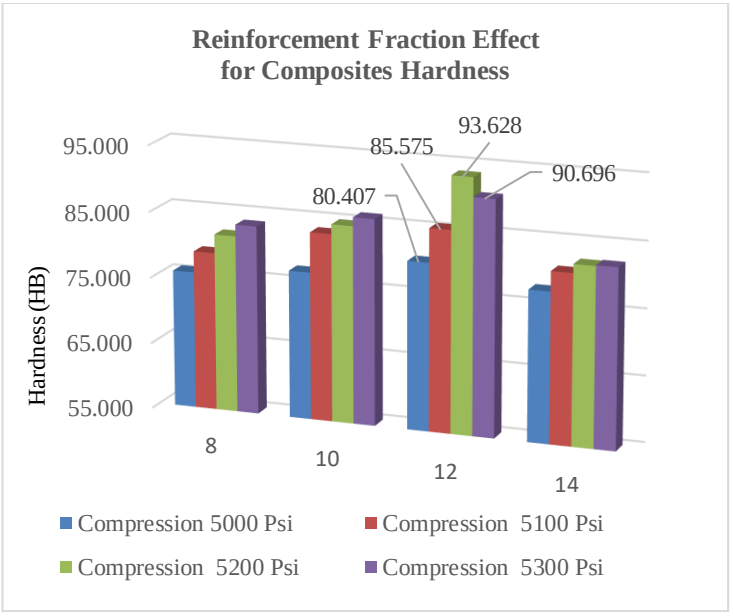

Fig. 2. Graph of NOB brake pad composite hardness

3.3 Wear

Wear testing was conducted in accordance with ASTM G99-17, *Pin-On-Disc* [42]. The friction roll disc had a thickness of 27.5 mm, a rotation speed of 517 rpm, a friction test duration of 3 minutes, and a load of 2 kg. The friction roll material is made of hardened steel alloy with a hardness of 25 HRC and a surface roughness (Ra) of 4.57 µm. This hardness test was conducted at the *αβγ* Laboratory in Landungsari, Malang, East Java. The test results were then calculated using equations (2) and (3). To facilitate comparison of wear rates under different load conditions, the calculated volumetric wear rate *(V)* was multiplied by the actual test load of 2 kg of newtons (2 kg = 19.6 N), with calculation results are shown in Fig.3. Specific Wear Volume (*V*) Graph of Non-Asbestos Brake Pad Composites.

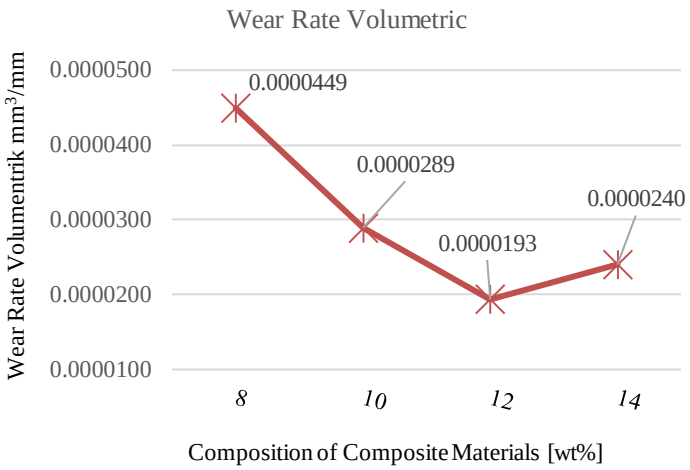

Fig. 3. Specific wear rate *(Vs)* graph for NOB brake pad composites

3.4 Microstrukture analysis

Characterization was performed *using Scanning Electron Microscopy* (SEM) to analyze the density and hardness of brake pad composites. Therefore, eight specimens showing higher density and hardness values were sent to the Indonesian Academy of Mechanical Engineering in Surakarta for SEM testing. The SEM results are shown in Fig. 4. Photo SEM of Non-Asbestos Brake Pad Composites with Reinforcements. A comparison of the four SEM images clearly indicates that the specimen with 12wt% reinforcement (Fig. 4(c)) has the fewest pores, cracks/fractures, or holes among the specimens. In other words, the *interlocking* bond phenomenon between particles and between the reinforcement powder and the matrix is more optimal. Meanwhile, the specimen with 8wt% reinforcement in Fig. 4. (a) and 10wt% in Fig. 4. (b) appear porous or has relatively many cracks/fractures or holes, and Fig. 4. (d), with a composite composition of 14wt%, there are clearly much larger cracks/fractures, so that when the hardness test is performed, it can affect the hard surface and affect the relatively soft hole groove.

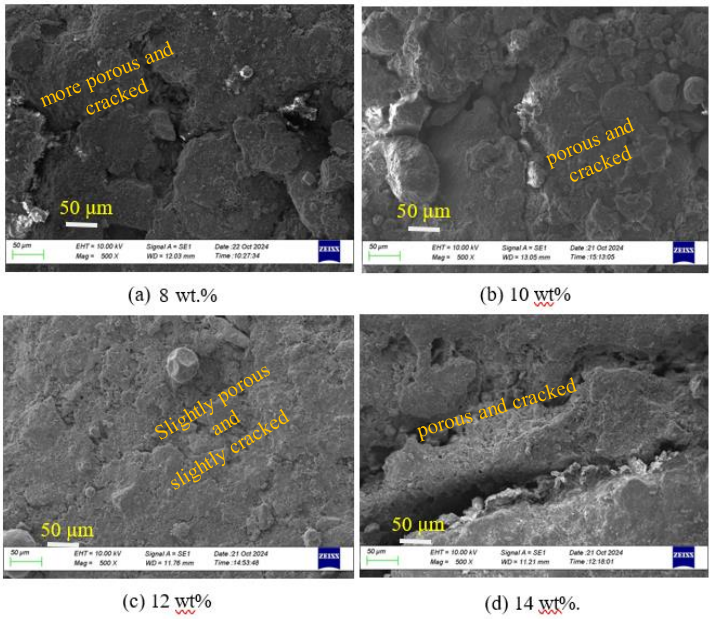

Fig. 4. Foto SEM of NOB brake pad composites with reinforcements: (a) 8%, (b) 10%, (c) 12%, and (d) 14%

In Fig. 4 (d) (14wt%), weak point of the matrix, which provides the bond between the reinforcement and the matrix, and this shows the occurrence of a weak point in the matrix's ability to provide its bonds. In the matrix toward the reinforcement have begun to decrease, and ultimately, very little *interlocking* bond can occur between the reinforcement and the matrix. This unfavorable condition also occurs even when the compaction pressure is increased from 5200 PSI to 5300 PSI. Therefore, based on the density, hardness, and wear-rate tests, this specimen exhibits high density and hardness and the lowest specific wear rate among the specimens.

Based on the varying pressure conditions, microstructure characterization with SEM photos was also carried out, with the results as shown in Fig. 5. The SEM photo characterization shown in Fig. 5, respectively, is a variation of compaction of 5000, 5100, 5200, and 5300 PSI., where the density of the specimen increases along with compaction, but at excessive compaction pressure, the density can decrease. This is most likely due to slippage in the particles. Comparison of SEM photos clearly shows that specimen (a) has a higher porosity than specimen (b), specimen (b) has a lower porosity than specimen (d), and specimen (c) has a lower porosity than specimen (d). In specimen sample (d), agglomeration occurs because there is too much reinforcing powder, so that the bond does not become stronger, but shows a decrease. In other words, the density, hardness, and wear rate of specimen (c) are better than the other three specimens. This indicates that the interlocking bond between the matrix powder and the reinforcing powder in specimen (c) is the best.

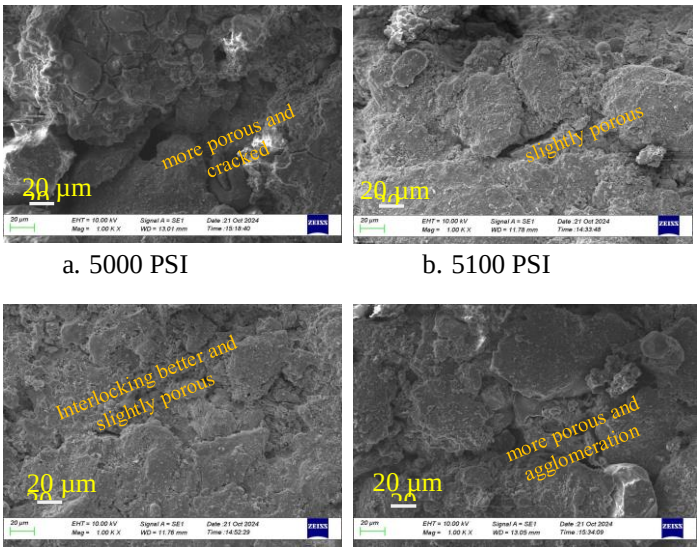

Fig. 5. Photo SEM tests of NOB brake pad composites with compaction pressure: (a). 5000 PSI, (b). 5100 PSI, (c). 5200 PSI, and (d). 5300 PSI.

The research comparison results for AMC-based NOB brake pads are shown in Table 3. Results Comparison of Several NOB Brake Pads. Based on the table, the density test results in this research paper fall in the middle among other AMC researchers, ranking higher than Research Choudhury [26] and lower than Research Subarmono [32] and Daniel-Mkpume [33]. While the hardness test results are above those of Choudhury [26] and Shaikh [34], they are below those of researchers Subarmono [32] and Daniel-Mkpume [33]. While the Wear Rate test results have higher wear resistance than those of three other researchers, Choudhury [26], Daniel-Mkpume [33] and Shaikh [34]. However, this paper is still superior to other researchers, because it uses reinforcement from a mixture of silica sand and BA and uses AMC from waste from Recycled Aluminum, so that by using this waste, the NOB brake pad composite research results in this paper are relatively cheaper or more competitive in the local brake pad market.

Table 3. Results comparison of several NOB brake pads.

Properties	Formulated AMC+12% (Silica S. +BA)	Formulated (Al-Si) + 12,5%. BA [26][32]	Formulated (AMC)+ 10%.BA [32] [39]	Formulated AMC + 10%. Silica S. [33] [40]	Formulated AMC + Silica S. +SIC [34] [41]
Densiy [g/cm^3]	2,121	1,85	≈ 2,55	2,6	2,48
Hardness [HB]	93,63	69,5	98,8	≈ 150	63
Wear Rate Volumetric [mm^3/mm]	0,0000193	0,005	0,0000226	Not – Available	0,000685

4 Conclusion

Referring to the results and discussion above, the best physical and mechanical properties for BA and Silica Sand Alloy reinforced composites were obtained with a reinforcement weight fraction of 12%, and the optimal compaction pressure was 5200 PSI. The details of this specimen are a hardness value of 93.628 HB, a density of 2.121 grams/cm³, and a specific wear rate value of 0.0193 mm³/Nm. After being converted to the SNI-09-0143-1987 standard requirements for two-wheeled motorcycle brake pads, the results of this study are within the tolerance limits, especially the hardness range of 65-105 HB and the density of 1.5-2.5 grams/cm³. Thus, it can be concluded that the findings of this study are that by adding BA and SiO_2 reinforcements to aluminum matrix composites, it is able to improve the mechanical capabilities of the composite and meet the brake pad standards. In addition, the most important finding of this research is that the composite produced does not use asbestos powder (NOB), but uses recycled aluminum as a matrix with reinforcement using a mixture of BA waste powder and silica powder from tin mining waste, so it is more environmentally friendly. In addition to the aluminum matrix, phenolic resin also has sufficient temperature resistance to meet the heat standards for motorcycle brake pads. However, this type of resin has a lower density than brake pads, requiring a balanced metal powder to provide reinforcement, such as brass powder, iron powder, copper powder, and others.

References

[1] Takahashi (ADDRI), "Asbestos-related disease," ADDRI, Concord Hospital, Gate 3 Hospital Road, Concord NSW 2139, Australia, 2026. https://addri.org.au/etoolkit/asbestos-related-disease/

[2] A. D. Lestari, N. Hairunisa, and A. M. Ridwan, "Occupational asbestos related diseases in Indonesia: A call for urgent action and awareness," *Jurnal Biomedika dan Kesehatan*, vol. 6, no. 2, pp. 224–234, Aug. 2023. https://www.jbiomedkes.org/index.php/jbk/article/view/402

[3] T. K. Ervik, S. E. Hammer, N. P. Skaugset, and P. Graff, "Measurements of airborne asbestos fibres during refurbishing," *Annals of Work Exposures and Health*, vol. 67, no. 8, pp. 952–964, 2023, doi:10.1093/annweh/wxad04.

[4] N. Van Zandwijk, G. Reid, and A. L. Frank, "Asbestos-related cancers: The 'hidden killer' remains a global threat," *Expert Review of Anticancer Therapy*, vol. 20, no. 4, pp. 271–278, 2020, doi: 10.1080/14737140.2020.1745067.

[5] D. Arachi, S. Furuya, A. David, A. Mangwiro, O. Chimed-Ochir, K. Lee, P. Tighe, J. Takala, T. Driscoll, and K. Takahashi, "Development of the 'National Asbestos Profile' to eliminate asbestos-related diseases in 195 countries," *International Journal of Environmental Research and Public Health*, vol. 18, art. no. 1804, 2021. https://www.ncbi.nlm.nih.gov/pmc/articles/PMC7917934.

[6] M. S. P. Boyles, C. A. Poland, J. Raftis, and R. Duffin, "The toxicology of chrysotile-containing brake debris: implications for mesothelioma," *Crit. Rev. Toxicol.*, vol. 49, no. 1, pp. 11–35, 2019. https://doi.org/10.1080/10408444.2019.1568385

[7] S. K. Hemanth and E. R. Dhas, "Development of eco-friendly brake pads using oil residue materials: Assessment of mechanical properties, biodegradation, and environmental impact," *Global NEST J.*, vol. 27, no. 6, p. 07399, 2025. https://doi.org/10.30955/gnj.07399

[8] X. Rong, D. Zhao, C. He, et al., "Review: recent progress in aluminum matrix composites reinforced by in situ oxide ceramics," *J. Mater. Sci.*, vol. 59, pp. 9657–9684, 2024. https://link.springer.com/article/10.1007/s10853-023-09120-z

[9] W. Zuliantoni, W. Suprapto, P. H. Setyarini, and F. Gapsari, "Hydroxyapatite-reinforced Al-Mg composites for corrosion resistance in hanks' balanced salt solution," *J. Polimesin*, vol. 22, no. 6, Dec. 2024. https://e-jurnal.pnl.ac.id/polimesin/article/view/5473.

[10] Sukanto, W. Suprapto, R. Soenoko, and Y. S. Irawan, "The effect of milling time on the alumina phase transformation in the AMCs powder metallurgy reinforced by silica-sand-tailings," *Eureka: Physics and Engineering*, vol. 1, pp. 103–117, Jan. 2022, https://journal.eujr.eu/engineering/article/view/1906.

[11] P. Garg, A. Jamwal, D. Kumar, K. K. Sadasivuni, C. M. Hussain, and P. Gupta, "Advance research progresses in aluminium matrix composites: manufacturing & applications," *J. Mater. Res. Technol.*, vol. 8, no. 5, pp. 4924–4939, Sep. 2019. https://doi.org/10.1016/j.jmrt.2019.06.028

[12] V. Buch, C. Patel, and V. Bhatt, "Matrix material selection framework for aluminium-based composites using fuzzy-AHP and TOPSIS," *Discover Mechanical Engineering*, vol. 5, 2026, doi: 10.1007/s44245-026-00200-3.

[13] B. Praveenkumar and S. D. Gnanaraj, "Case studies on the applications of phenolic resin-based composite materials for developing eco-friendly brake pads," *J. Inst. Eng. India Ser. D*, vol. 101, pp. 327–334, 2020. https://doi.org/10.1007/s40033-020-00231-4

[14] J. Liu, J. Guo, J. Deng, S. Fan, X. Cai, S. Kou, and S. Yang, "Preparation and properties of boron modified phenolic resin for automotive friction materials," *Materials*, vol. 18, 2025, https://doi.org/10.3390/ma18071624.

[15] Standar Nasional Indonesia, SNI 09-0143-1987: *Standar Kampas Rem Kendaraan Bermotor*, Jakarta, Indonesia, 1987. https://www.scribd.com/document/425491959/SNI-09-0143-1987-Kampas-Rem-Kendaraan-Bermotor.

[16] Standar Nasional Indonesia, SNI.09-4404-2008, *Standar Kampas Rem Mobil dan Motor (Terbaru)*, Standar Kampas Rem Mobil dan Motor | PDF.

[17] DV Dudina dan AV Ukhina, "Powder Metallurgy: Materials and Processing," *Materials*, vol. 16, no. 13, 4575, 2023, https://doi.org/10.3390/ma16134575.

[18] G. Mathew dan VK Kottur, "A review on the reinforcement of aluminium composites using industrial waste materials: Enhancing mechanical properties and tribological performance," *Next Materials*, vol. 9, Art. no. 101356, Okt. 2025, https://doi.org/10.1016/j.nxmate.2025.101356.

[19] D. A. Gok, C. Bayraktar, and M. Hoskun, "A review on processing, mechanical and wear properties of Al matrix composites reinforced with Al2O3, SiC, B4C and MgO by powder metallurgy method," *J. Mater. Res. Technol.*, vol. 31, pp. 1132–1150, 2024. https://doi.org/10.1016/j.jmrt.2024.06.110

[20] C. Suryanarayana, "Mechanical alloying: a critical review," *Mater. Res. Lett.*, vol. 10, no. 10, pp. 619–647, 2022. https://doi.org/10.1080/21663831.2022.2075243.

[21] S. K. Selvaraj, R. Ramesh, T. M. V. Narendhra, I. N. Agarwal, U. Chadha, and V. Paramasivam, "New developments in carbon-based nanomaterials for automotive brake pad applications and future challenges," *J. Nanomater.*, vol. 22, 2021, pp. 1–24. https://www.hindawi.com/journals/jnm/2021/6787435/

[22] S. Oyelami, A. A. Adefajo, A. E. Okeleye, A. T. Oyewo, A. S. Adedutan, and A. L. Ajao, "A review on rice husk ash as a sustainable reinforcement in aluminium, process and applications," *Adeleke Univ. J. Eng. Technol. [AUJET]*, vol. 8, no. 1, pp. 240–252, 2025. https://aujet.adelekeuniversity.edu.ng/index.php/aujet/article/view/540

[23] S. S. Barve and H. P. Khairnar, "Use of rice husk and sugarcane bagasse ash for development of automotive brake pad friction material," *EVERGREEN J. Novel Carbon Res. & Green Asia Strategy*, vol. 12, no. 1, pp. 27–40, Mar. 2025. https://www.tj.kyushuu.ac.jp/evergreen/contents/EG2025-12_1_content/pdf/p27-40.pdf

[24] A. M. Razzaq, D. L. Majid, U. M. Basheer, dan H. S. S. Aljibori, "Research summary on the processing, mechanical and tribological properties of aluminium matrix composites as effected by fly ash reinforcement," *Crystals*, vol. 11, no. 10, p. 1212, 2021, doi: 10.3390/cryst11101212.

[25] A. S. Abood, J. P. K., G. Karuna, A. Jain, R. Goel, and P. K. Chandra, "Advancing aluminum-based composites with fly ash and SiC reinforcement through stir casting," *E3S Web Conf.*, vol. 507, art. no. 01050, 2024. https://doi.org/10.1051/e3sconf/20245070105.

[26] A. Choudhury, J. Nanda, and S. N. Das, "Enactment of aluminium-fly ash composites," *J. Phys.: Conf. Ser.*, vol. 1706, p.012138, 2020, https://iopscience.iop.org/article/10.1088/1742-6596/1706/1/012138/pdf

[27] S. Bakri, M. A. Abdullah, M. I. Juradi, and S. R. Nurhawaisyah, "Study of SiO_2 separation in silica sand using shaking table," *Jurnal Inovasi Pertambangan dan Lingkungan*, vol. 3, no. 2, pp. 85–91, 2023, https://journal.uinjkt.ac.id/index.php/jipl/article/viewFile/34225/pdf

[28] P. Lestari, R. A. Berliani, E. A. Pratama, R. A. Al-Jannata, D. V. Pratiwi, and H. Widiyandari, "Extraction of silica (SiO_2) from rare-earth metal zircon ($ZrSiO_4$) as lithium-ion battery anode material," *J. Kim. Sains dan Aplikasi*, vol. 26, no. 3, pp. 79–84, May 2023. https://doi.org/10.14710/jksa.26.3.79-84

[29] A. M. Syahrani, R. Juniah, Syarifudin, H. Rahmi, and Syaifudin, "Analysis of increasing silica sand content using a magnetic separator to meet the needs of the safety glass industry," *Jurnal Sains dan Teknologi*, vol. 24, no. 1, pp. 13–21, 2024. https://doi.org/10.36275/gh9wja94

[30] S. Sukanto, R. Soenoko, W. Suprapto, and Y. S. Irawan, "Characterization of aluminium matrix composite of Al-ZnSiFeCuMg alloy reinforced with silica sand tailings particles," *J. Mech. Eng. Sci.*, vol. 14, no. 3, pp. 7094–7108, Sep. 2020. https://journal.ump.edu.my/jmes/article/view/2867/873.

[31] V. E. Ogbonna, O. M. Popoola, A. P. I. Popoola, et al., "Evaluation of the microstructural, mechanical, tribological, and corrosion properties of zinc-based composites reinforced silica beach sand particulates," *J. Bio Tribo Corros.*, vol. 11, p. 26, 2025. https://link.springer.com/article/10.1007/s40735-025-00949-2

[32] Subarmono, Jamasri, M. W. Wildan, dan Kusnanto, "Utilization of fly ash waste as reinforcement of aluminium matrix composite produced using powder metallurgy," *Jurnal Manusia dan Lingkungan*, vol. 18, no. 2, pp. 98–104, Jul. 2011, doi:10.22146/jml.18814.

[33] C. C. Daniel-Mkpume, E. G. Okonkwo, V. S. Aigbodion, P. O. Offor, dan K. C. Nnakwo, "Silica sand modified aluminium composite: An empirical study of the physical, mechanical and morphological properties," *Materials Research Express*, vol. 6, 076539, 2019, doi: 10.1088/2053-1591/ab14c6

[34] M. B. N. Shaikh, S. Arif, and M. A. Siddiqui, "Fabrication and characterization of aluminium hybrid composites reinforced with fly ash and silicon carbide through powder metallurgy," *Materials Research Express*, vol. 5, no. 4, p. 046506, 2018, doi: 10.1088/2053-1591/aab829.

[35] F. Hasbi, Sukanto, and Erwanto, "Pengaruh variasi fraksi penguat dan suhu sintering AMC terhadap nilai densitas dan kekerasan dengan penguat SiO_2/RHA/BA," *Machine: Jurnal Teknik Mesin*, vol. 11, no. 1, Apr. 2025, doi: 10.33019/jm.v11i1.5871.

[36] N. Kumar, A. Bharti, and K. K. Saxena, "A re-investigation: Effect of powder metallurgy parameters on the physical and mechanical properties of aluminium matrix composites," *Materials Today: Proceedings*, vol. 44, pt. 1, pp. 2188–2193, 2021, https://doi.org/10.1016/j.matpr.2020.12.351.

[37] ASTM E110, *Standard Test Method for Rockwell and Brinell Hardness of Metallic Materials by Portable Hardness Testers*, ASTM B. Stand., pp. 4–8, 2015, doi: 10.1520/E0110-14.2xx.

[38] I. A. Wahyudie, R. Soenoko, W. Suprapto, and Y. S. Irawan, "Enhancing hardness and wear resistance of ZrSiO4-SnO2/Cu10Sn composite produced by warm compaction and sintering," *Metalurgija*, 2019. https://hrcak.srce.hr/file/327708

[39] L. Cao, Q. Dai, Q. Liang, and X. Zhang, "The influence of process conditions and reinforcement characteristics on the densification and mechanical properties of powder metallurgy SiCp/Al composites," *Materials*, vol. 18, p. 5060, 2025, https://doi.org/10.3390/ma18215060

[40] K. C. Nayak, K. K. Rane, P. P. Date, and T. S. Srivatsan, "Synthesis of an aluminum alloy metal matrix composite using powder metallurgy: Role of sintering parameters," *Applied Sciences*, vol. 12, no. 17, p. 8843, 2022, https://doi.org/10.3390/app12178843.

[41] ASTM International, *Standard Test Methods for Density of Compacted or Sintered Powder Metallurgy (PM) Products Using Archimedes' Principle*, ASTM B962-17, vol. I, pp. 1–7, 2013, doi: 10.1520/B0962-17.2.

[42] ASTM G99-17, *Standard Test Method for Wear Testing with a Pin-on-Disk Apparatus*, ASTM International, West Conshohocken, PA, 2023. https://www.astm.org/g0099-17.html.

[43] A. Multazam, W. Suprapto, and Pratikto, "The effect of temperature in the hot isostatic pressing process on porosity, wear, and microstructure of duralumin sludge powder," *J. Rekayasa Mesin*, vol. 5, no. 3, pp. 209–216, 2015., https://media.neliti.com/